Science Advances

18 DECEMBER 2020

AAAS

OCEANOGRAPHY

Modeling the breakup of tabular icebergs

Mark R. England[1,2]*, Till J. W. Wagner[1], Ian Eisenman[2]

Nearly half of the freshwater flux from the Antarctic Ice Sheet into the Southern Ocean occurs in the form of large tabular icebergs that calve off the continent's ice shelves. However, because of difficulties in adequately simulating their breakup, large Antarctic icebergs to date have either not been represented in models or represented but with no breakup scheme such that they consistently survive too long and travel too far compared with observations. Here, we introduce a representation of iceberg fracturing using a breakup scheme based on the "footloose mechanism." We optimize the parameters of this breakup scheme by forcing the iceberg model with an ocean state estimate and comparing the modeled iceberg trajectories and areas with the Antarctic Iceberg Tracking Database. We show that including large icebergs and a representation of their breakup substantially affects the iceberg meltwater distribution, with implications for the circulation and stratification of the Southern Ocean.

INTRODUCTION

Large tabular icebergs are one of the dominant sources of freshwater discharge into the Southern Ocean. Recent estimates, from a combination of satellite observations and ice sheet models (*1*, *2*), indicate that approximately half (~1300 Gt/year) of the total flux of fresh water from the Antarctic Ice Sheet to the Southern Ocean (~2750 Gt/year) is delivered by icebergs that calve from the ice sheet's glaciers and ice shelves. The vast majority of the iceberg flux is contained in giant tabular icebergs: Tournadre *et al.* (*3*) estimated that nearly 1000 Gt/year of fresh water is delivered by icebergs that have horizontal lengths over 18 km, even though these account for less than 4% of the total number of Antarctic icebergs. More recently, Tournadre *et al.* (*4*) found that 95% of iceberg volume is contained in icebergs with horizontal areas larger than 5 km^2. However, while some progress has been made on including small icebergs in fully coupled modeling frameworks (*5*–*10*), the current generation of climate models (CMIP6) do not include any representation of large tabular icebergs.

Previous studies have shown that models lacking a representation of icebergs will introduce systematic biases in their simulation of the southern high-latitude climate (*5*–*9*, *11*–*13*). Icebergs affect the Southern Ocean primarily by transporting large amounts of fresh water away from the Antarctic coast and then distributing it into the upper few hundred meters of the open ocean. The response of the circulation and stratification of the Southern Ocean is expected to be highly sensitive to the location and rate of this freshwater input. For example, a large amount of fresh water added over the continental shelf could limit the production of Antarctic Bottom Water (*12*, *14*). A more moderate addition of fresh water in the same location could instead only result in fresher Antarctic Bottom Water (*15*). Alternatively, fresh water deposited in the open ocean may affect the Antarctic Circumpolar Current (ACC) through changes to the surface buoyancy forcing (*16*). In addition to being sources of fresh water, icebergs take up a large amount of latent heat as they melt, which has potential implications for Antarctic sea ice cover (*5*, *8*) and also for the stability of the Antarctic Ice Sheet (*17*). Therefore, it is important to be able to simulate the evolution of large tabular icebergs so as to accurately model the distribution of nearly half of the total freshwater flux from the Antarctic Ice Sheet to the Southern Ocean and its resulting climate impacts.

Beyond the current climate, improvements in the representation of tabular icebergs will further our ability to model both past and future climates. One example is the modeling of Heinrich events (*18*, *19*), where, during previous glacial periods, icebergs are believed to have calved from the glacial ice sheet in North America in large numbers and traversed the North Atlantic, possibly interacting with sea ice (*20*) and other elements of the climate system. With regard to the future, iceberg calving rates are expected to increase during the coming century in step with rising overall rates of ice sheet mass loss (*21*, *22*). Accordingly, the climate impacts of icebergs may become more prominent under continued global warming.

Yet, there is a crucial shortcoming in previous iceberg modeling studies: They do not accurately simulate the evolution and trajectories of large icebergs. Here, we define large icebergs as Antarctic icebergs with horizontal area greater than 3 km^2, which is larger than all icebergs in the size distributions of Gladstone and Bigg (*23*) and Merino *et al.* (*8*) that have been widely used in modeling studies. There are two main approaches in previous studies regarding the simulation of large icebergs, both with crucial weaknesses:

1) Most studies simply ignore large icebergs and only simulate the effects of icebergs smaller than 3 km^2, which they treat either explicitly (*5*–*9*, *13*, *23*) or implicitly through prescribed meltwater fluxes (*12*, *14*, *24*). Given that icebergs larger than 3 km^2 account for more than 95% of all ice mass calved from the Antarctic Ice Sheet and that observational studies have shown that tabular icebergs are subject to different dynamics than smaller icebergs (*25*–*27*), this is a notable shortcoming.

2) Rackow *et al.* (*11*) and Wagner *et al.* (*28*) (hereafter referred to as WDE17), by contrast, explicitly include large tabular icebergs but do not include representations of the iceberg breakup. As a result, the simulated large icebergs survive for far too long once in open water compared to observations (see "Proposed Model of Iceberg Breakup" section). A basic problem with this approach is that meltwater is introduced into regions where no icebergs have ever been detected. To avoid this issue, WDE17 only simulate the trajectories of large Antarctic icebergs for the first year. We note that the simulation of Arctic icebergs does not face the same challenges because, in the modern climate, large tabular icebergs are found almost exclusively in the Southern Hemisphere.

In light of these issues, it has been previously suggested that current iceberg models are missing a key physical process necessary

[1]Department of Physics and Physical Oceanography, University of North Carolina Wilmington, Wilmington, NC, USA. [2]Scripps Institution of Oceanography, University of California San Diego, La Jolla, CA, USA.
*Corresponding author. Email: mengland@ucsd.edu

for simulating large tabular icebergs: a representation of breakup (*4*). Here, we present an approach for modeling the breakup of large tabular icebergs via repeated fracture, or "edge wasting" [a term coined by Scambos *et al.* (*26*)]. This process, which we represent stochastically, is based on a physical iceberg breakup mechanism. We explore this using an analytical iceberg drift model, and we show that when we include breakup through the proposed fracturing representation, the resulting simulated iceberg trajectories and areas are much closer to observations. Last, we show that incorporating this representation of fracturing has a substantial impact on the resulting meltwater distribution, and we demonstrate how previous methods of modeling Antarctic icebergs produce large biases in the meltwater distributions.

METHODS

Observational data

Database of tabular icebergs 1992–2019

For an observational estimate of the trajectories of large icebergs over the past three decades, we use the consolidated Brigham Young University National Ice Center (BYU/NIC) Antarctic Iceberg Tracking Database, detailed in Budge and Long (*29*). This database includes daily estimates of the location of icebergs with areas larger than 5 km^2 derived from scatterometer data for the period 1992 to present. These trajectories are shown in Fig. 1. We also use previous in-depth analyses of several individual icebergs [B17a and C19a (*30*), as well as C28a and C28b (*31*)].

Iceberg calving

Estimates of observed iceberg calving rates from different ice shelves are taken from Merino *et al.* (*8*), based on the work of Depoorter *et al.* (*1*). Figure S1 shows the calving rates at each discharge location. For simplicity, we use the same size distribution at all calving sites, following Merino *et al.* (*8*). The accuracy of this simplification is somewhat difficult to assess because of the relative paucity of large tabular icebergs in the observed record.

Iceberg simulations

Analytical drift model of WDE17

We use the analytical model of WDE17 to simulate the evolution of Antarctic icebergs. This model, adapted from the canonical iceberg model of Bigg *et al.* (*32*), computes the iceberg velocity $\boldsymbol{v}_i$ from the ocean current velocity $\boldsymbol{v}_w$ and the surface wind velocity $\boldsymbol{v}_a$

$$\boldsymbol{v}_i = \boldsymbol{v}_w + \gamma(-\alpha\hat{\boldsymbol{k}} \times \boldsymbol{v}_a + \beta\boldsymbol{v}_a) \quad (1)$$

Here, γ represents sensitivity to wind relative to ocean currents and is computed from the water and air drag coefficients and the water, air, and iceberg densities, and we use a constant value of γ = 0.019 (or ≈2%). The coefficients α and β are functions of iceberg size, wind speed, and the Coriolis parameter, and they determine the relative importance of the cross-wind and along-wind components of the iceberg drift. See WDE17 for further details. We note that this drift model does not include the effects of sea ice drag (although the effects of sea ice are included in the decay model in the "Decay Parameterizations" and "Proposed Model of Iceberg Breakup" sections), which is an important limitation to this study (*33*).

When $\alpha \ll \beta$, which applies for small icebergs or strong winds, icebergs approximately follow the "2% rule": They drift at 2% of the wind velocity relative to the ocean current. On the other hand, when $\alpha \gg \beta$, which applies for large tabular icebergs or when winds are weak, icebergs drift with the ocean current.

WDE17 demonstrate that this model simulates the trajectories of both Arctic and Antarctic icebergs well compared to observations. The model allows the efficient computation of thousands of iceberg trajectories, which is helpful here because simulating large numbers of these icebergs provides an estimate of the mean freshwater response, without being influenced by individual icebergs, which can be a challenge in more computationally expensive models.

Input data

The model is forced with high-resolution daily data for sea surface temperature (SST), ocean currents, and surface winds. Note that these forcing fields are noninteractive: Icebergs do not influence the climate in these simulations. We focus on the years for which there are comprehensive observations of large icebergs, 1992–2019. Climatological values of the input fields are shown in fig. S2. Note that all data are first regridded onto a common 1/4° grid.

For the ocean variables (SST, currents, and sea ice concentration), we use the Estimating the Circulation and Climate of the Ocean version 2 (ECCO2) product (*34*). ECCO2 is a high-resolution global ocean and sea ice state estimate that uses a model fit to available satellite and in situ observational data. It covers the years 1992 to present. It uses a cubed sphere grid with a horizontal resolution of 18 km. ECCO2 has been shown to accurately simulate Southern Ocean SST (*34*), the ACC (*35*), and Antarctic sea ice cover (*36*) compared to observations, although the simulated sea surface salinity in the Southern Ocean is biased salty (*37*).

Figure S2A shows the zonal component of the upper 200-m average ocean current. The upper 200-m average is used because previous studies have shown that the iceberg trajectories are influenced by the currents over the full depth of the iceberg (*8*), which is typically around a couple of hundred meters for the icebergs that we model. The two main features to note are the strong west-to-east flow of the ACC and the countercurrent close to the coastline of Antarctica. Having a high-resolution ocean state estimate that can capture this countercurrent is important because it is this that pushes the large icebergs westward around the continent (Fig. 1). The meridional currents close to Antarctica (fig. S2B) are small but typically direct the icebergs poleward, which helps explain why observed icebergs stay so close to the coastline (Fig. 1).

We use ERA5 reanalysis (*38*) for the near-surface wind conditions (fig. S2, D and E). ERA5 is an hourly, high-resolution atmospheric reanalysis product on a 30-km grid that covers the time period 1950 to present. Previous studies have shown that the ERA5 surface wind estimates outperform other reanalysis products, both globally (*39*) and specifically near Antarctica (*40*). Over the Southern Ocean, the main climatological surface wind feature is the strong westerlies (fig. S2D), while the meridional winds are much weaker (fig. S2E).

Iceberg size distributions

As discussed in the Introduction, most previous studies have not included icebergs with horizontal areas larger than 3 km^2 and have typically used the iceberg size distribution from Gladstone and Bigg (*23*) (Fig. 2 and table S1, referred to hereafter as the "Gladstone distribution"), which is an updated version of the Bigg *et al.* (*32*) distribution. However, more recently, Tournadre *et al.* (*4*) demonstrated that the size distribution of observed Antarctic icebergs instead follows a −1.5 power law, with icebergs under 3 km^2 accounting for

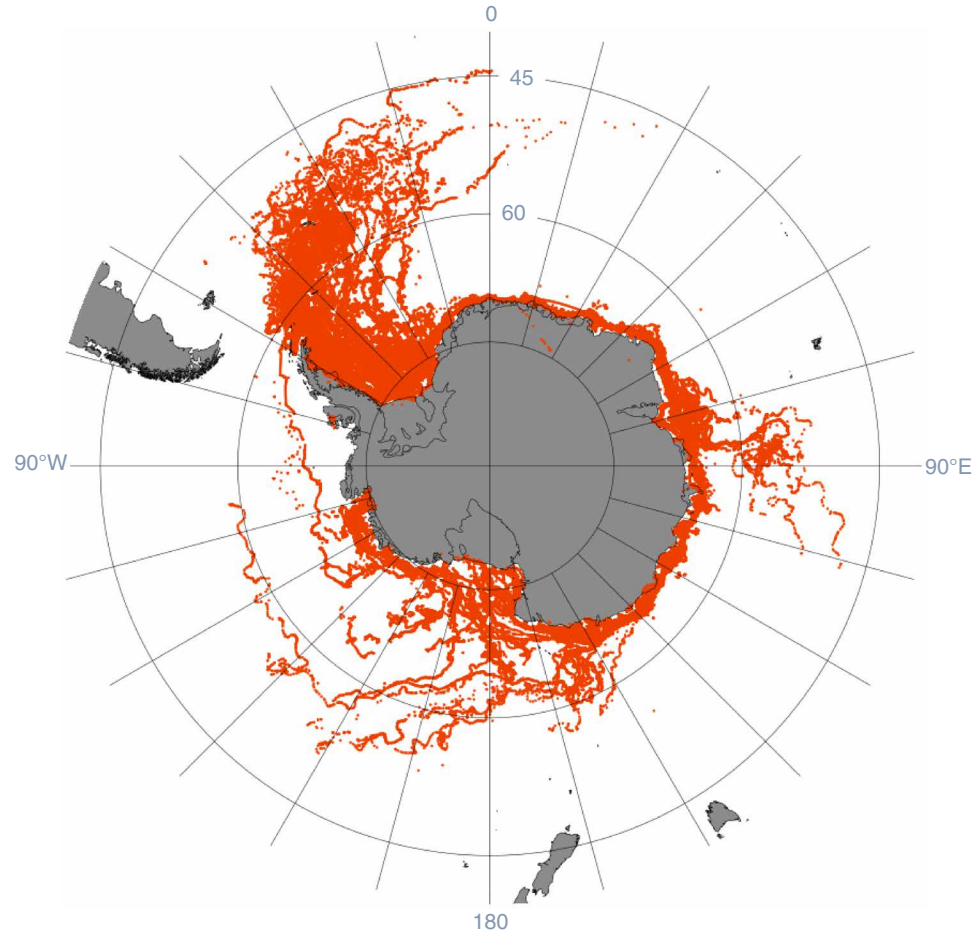

Fig. 1. Observed positions of tabular Antarctic icebergs. Daily positions of Antarctic icebergs larger than 5 km^2 for the period 1992–2019 from the BYU/NIC database.

less than 5% of the total calved iceberg volume. Figure 2 and table S2 show the size distribution we have created for this study, hereafter referred to as the "power law distribution." The power law distribution follows a −1.5 power law, with sizes ranging from 0.3 to 1000 km^2. We do not include icebergs smaller than 0.3 km^2 because these account for less than 0.5% of the total iceberg volume. In addition, we have not included the gigantic icebergs larger than 1000 km^2 that are occasionally observed. The size distribution of Tournadre *et al.* (*4*) suggests that only 0.4% of all icebergs are this large. Although these rare gigantic icebergs account for a substantial fraction of the total iceberg volume (*4*), we do not explicitly include them in this study. However, these gigantic icebergs typically break into pieces smaller than 1000 km^2 shortly after calving, long before they enter the open ocean (e.g., icebergs B15, A43, and A48). We discuss this further in the Discussion section. We emphasize that the power law distribution used here is much more observationally consistent for Antarctic icebergs than the Gladstone distribution used in previous studies. The implications of using such a different distribution are discussed in the "Effects on iceberg trajectories and meltwater distribution" section.

Decay parameterizations

In WDE17, the drift model (summarized above) is coupled to a decay model that is adapted from the decay representation of Bigg *et al.* (*32*). Three iceberg melt processes are accounted for in most modeling studies in slightly varying forms: (i) wind-driven wave erosion, (ii) sidewall erosion from buoyant convection, and (iii) turbulent basal melt. Here, we largely adopt the formulation of WDE17. The parameterized equations are as follows

$$\frac{dL}{dt} = \frac{dW}{dt} = -\frac{1}{2}(1+\cos\pi C^3)\left(a_1 |\boldsymbol{v}_a|^{\frac{1}{2}} + a_2 |\boldsymbol{v}_a|\right) - (b_1 T_w + b_2 T_w^2)\Theta(T_w) \quad (2)$$

$$\frac{dH}{dt} = -c\,|\boldsymbol{v}_w - \boldsymbol{v}_i|^{\frac{4}{5}}(T_w - T_i)L^{-\frac{1}{5}} \quad (3)$$

where the dimensions of the tabular iceberg are length (L), width (W), and thickness (H); the parameter values are $a_1 = 8.7 \times 10^{-6}$ m$^{\frac{1}{2}}$ s$^{-\frac{1}{2}}$, $a_2 = 5.8 \times 10^{-7}$, $b_1 = 8.8 \times 10^{-8}$ ms^{-1} K^{-1}, $b_2 = 1.5 \times 10^{-8}$ ms^{-1} K^{-2}, $c = 6.7 \times 10^{-6}$ m$^{-\frac{2}{5}}$ s$^{\frac{1}{5}}$ K^{-1}; T_w is the SST, and $T_i = -4$°C is the ice temperature, both expressed as departures from the freshwater melting point; C is the fractional sea ice concentration; and Θ is the Heaviside function. The first term on the right-hand side of Eq. 2 is a parameterization of the wind-driven wave erosion, and the second is a parameterization of the sidewall erosion from buoyant convection. Note that because both of these decay processes are suppressed by sea ice, we have adapted the wind-driven wave erosion term from Martin and Adcroft (*6*) to include an explicit dependence on sea ice concentration, and the sidewall erosion term is set to zero when

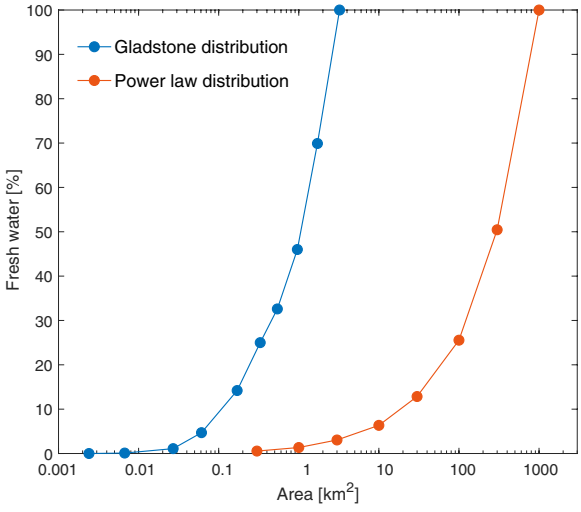

Fig. 2. Iceberg size distributions used in the simulations. Cumulative distribution of total freshwater input for each size class of iceberg area following the Gladstone distribution of small Antarctic icebergs (blue) and the power law distribution (red) based on the −1.5 power law (*4*). The iceberg area is shown on a log scale. Further details regarding the dimensions of the different size classes for the two distributions can be found in tables S1 and S2.

$T_w < 0$. The right-hand side of Eq. 3 is a parameterization of turbulent basal melt. Surface melt and air forced convection have been found in previous studies to minimally contribute to iceberg decay (*41*, *42*), and these processes have been neglected in the present model. Eqs. 2 and 3 determine the change in the three dimensions of the iceberg (W, L, and H) and thus together determine the rate of volume loss. Notably, this canonical decay model lacks any representation of breakup through fracturing.

Proposed model of iceberg breakup

The three processes outlined in the "Decay Parameterizations" section were established to model the decay of relatively small (typically Arctic) icebergs. However, Tournadre *et al.* (*3*) estimate that 80% of the decay of large tabular icebergs comes from breakup processes that produce much smaller icebergs. These icebergs are typically smaller than 5 km^2 and hence are below the detection threshold of the BYU/NIC database. This estimate, that a large fraction of the decay of tabular icebergs comes from breakup processes, is consistent with the ship-based observational study of Jacka and Giles (*43*).

There are multiple other lines of evidence that similarly suggest that the process of small icebergs fracturing off larger icebergs (i) occurs frequently in observations and (ii) is key for understanding the observed size distribution of Antarctic icebergs in the open ocean. First, small icebergs can be seen calving from the edges of larger icebergs in satellite imagery (*26*, *27*, *31*). Second, analysis of the evolution of individual tabular icebergs shows a discontinuous, step-like time series for the iceberg area (*30*, *44*), suggesting that smaller icebergs fracture off in discrete events. Third, Tournadre *et al.* (*4*) conclude that the −1.5 power law for Antarctic icebergs is due to the statistical properties of brittle fragmentation (*45*); in other words, the observed size distribution of icebergs in the open ocean is consistent with decay through brittle fragmentation rather than thermodynamic melting.

Despite this extensive evidence for the importance of breakup events for the decay of tabular icebergs, to date, the most widely used iceberg decay models have not included representations of iceberg breakup. We note that a representation of decay through the calving off of small slabs is included in the Canadian Ice Service model (*42*, *46*), although this was only applied to small Arctic icebergs and has not been widely adopted.

We focus our representation of iceberg breakup on the "footloose" mechanism, an edge-wasting process that was first outlined in Scambos *et al.* (*26*) and described in detail in Wagner *et al.* (*47*). This mechanism works as follows:

1) A combination of warm surface waters and wave action causes a wave-cut to form at the water line (fig. S3, step 1).

2) When the wave-cut reaches a critical depth, the overhanging cliff becomes unstable and collapses, leaving a protruding foot under the water line (fig. S3, step 2).

3) An unbalanced buoyancy force on the submerged protruding foot induces a torque on the iceberg, leading to a deformed edge profile (fig. S3, step 3).

4) The induced torque causes an internal stress field, and when the critical stress is reached (when the protruding foot is long enough), a smaller iceberg breaks off the main iceberg (fig. S3, step 4). The process begins again at step 1 on the newly exposed face of the large tabular iceberg.

This process gives a physical basis for the typical length-scale of the small iceberg that breaks off (*47*)

$$l = (\pi/2\sqrt{2})\, l_w$$

where l is the length of the broken off iceberg and

$$l_w = (B/g\rho_w)^{\frac{1}{4}}$$

is the buoyancy length, where $B = EH^3/12(1-\nu^2)$ is the bending stiffness of a beam of thickness H and Young's modulus E, ν is the Poisson ratio, g is the acceleration due to gravity, and ρ_w is the density of water. Therefore, l scales with the iceberg thickness H to the 3/4 power. For typical tabular iceberg thicknesses ($H \approx 200 - 400$ m), l is of the same order of magnitude as the iceberg thickness ($l \approx 320 - 550$ m). It is important to note that this process predominantly occurs in open water away from sea ice, because for this chain of events to unfold, a wave-cut needs to form first.

Here we add a stochastic representation of this footloose mechanism into the drift and decay model of WDE17. Every model time step Δt, we break off a number of small icebergs, k, according to a probability $P(k, \Delta t)$ from a Poisson distribution:

$$P(k,\Delta t) = \frac{(r\Delta t)^k e^{-r\Delta t}}{k!} \quad (4)$$

This introduces a new model parameter r that represents the average number of icebergs broken off per day. One key approximation is that this parameter r is constant. More discussion of this is included in the Discussion section. For large values of $r\Delta t$, this Poisson distribution approaches a normal distribution with a mean of $r\Delta t$ and a standard deviation of $\sqrt{r\Delta t}$. We refer to the large tabular iceberg as the "parent" iceberg, and the small icebergs that fracture from it as "child" icebergs. Further details of the breakup scheme are as follows: (i) breakup only occurs when the length of the parent iceberg, L, is greater than $3l$, which is approximately 900 m; (ii) k is reduced

until detail (i) is satisfied; (iii) breakup of the parent iceberg does not occur ($k = 0$) when $C > 0.5$, i.e., when there is more sea ice cover than open ocean, because the footloose mechanism is much less prevalent when an iceberg is surrounded by sea ice; (iv) when $k > 0$, the longer horizontal dimension (L) of the parent iceberg is reduced by $k(3l^2/W)$, while the shorter horizontal dimension (W) remains unchanged; (v) the child icebergs each start with dimensions $l \times 3l$, which is approximately 0.25 km^2; and (vi) the child icebergs do not themselves break up further by the footloose process because they are small. The choice of implementing a stochastic breakup scheme rather than a constant-rate breakup scheme visibly increases the variability of the trajectories of the small- to medium-size parent icebergs (with areas of 0.3 to 10 km^2 in table S2), but it has limited effects on the range of potential trajectories simulated for the larger parent icebergs (with areas of 100 to 1000 km^2 in table S2).

We keep track of the trajectory of each child iceberg because it is these smaller icebergs, rather than the lone parent iceberg, that deliver the bulk of the fresh water to the Southern Ocean (fig. S4). The importance of the parent icebergs lies in their acting as conveyor belts for the multitude of child icebergs: The trajectories of the large tabular icebergs determine where the small icebergs are released into the Southern Ocean and, therefore, where they ultimately deposit fresh water. As an example of the results of this breakup scheme, fig. S5 shows the trajectories of five large tabular icebergs (red) and the trajectories of their children (gray).

To demonstrate the effect of this breakup scheme, we simulate 10,000 individual 300-km^2 icebergs with and without the breakup scheme, and we compare the results with an observed iceberg of similar size, B17a (Fig. 3). Iceberg B17a formed as the larger B17, which originated from the Ross Sea Ice Shelf in 2000 (*48*) and then calved into several pieces near Cape Hudson in 2002 (68°S, 153°E). B17a continued its westward drift through sea ice around the coastline of the Antarctic for over a decade. It entered the open ocean in the Weddell Sea in 2014 and then deteriorated over a period of 15 months as it traveled northward (*30*). In Fig. 3, we show the daily evolution of iceberg area for B17a after entering the open ocean [black crosses, from (*30*)], which we compare with simulated icebergs without the breakup scheme (blue) and simulated icebergs using the breakup scheme with $r = 4$ breakups/day (orange). All of these icebergs enter the open ocean from the Weddell Sea region so they can be directly compared. Without the breakup scheme, the modeled icebergs survive in open water for ~25 to 30 years. These prolonged life spans [also noted in (*11*, *28*)] are clearly incompatible with the observed iceberg B17a and the other icebergs in the BYU/NIC database (*29*). This suggests that the traditionally modeled thermodynamic decay processes alone are insufficient to explain the observed rate of deterioration. By including the breakup scheme, the modeled icebergs only survive for between 1 and 3 years, consistent with observations. For icebergs the size of B17a, we find that the traditional melt terms contribute only ~10% of the total decay of tabular icebergs, with the breaking off of child icebergs contributing the remaining ~90%.

RESULTS

Effects on iceberg trajectories and meltwater distribution

Most previous studies of the effects of icebergs on the Southern Ocean have ignored large tabular icebergs. The total volume of ice calved was instead released as multitudes of small icebergs. In our first set of runs in which only small icebergs are released according to the Gladstone distribution, relatively few icebergs make it into the ACC (Fig. 4A), and the vast majority of the fresh water is injected close to the Antarctic coastline (Fig. 4D), consistent with the modeling results of Merino *et al.* (*8*).

However, given that the calving of small icebergs contributes less than 5% of the fresh water supplied by icebergs to the Southern Ocean, and given that small icebergs evolve rather differently than large icebergs, the validity of this meltwater distribution should be revisited.

Here, we present a second set of simulations in which large icebergs are included (according to the power law distribution), and the larger icebergs drift much further from the Antarctic continent. Without the breakup scheme (Fig. 4B), the larger icebergs drift for hundreds of kilometers in the Southern Ocean. Most icebergs survive in waters that are over 10°C and leave the domain (south of 40°S) before they are fully melted, which is not consistent with observations (Fig. 1). The resulting freshwater distribution (Fig. 4E) is fairly spatially uniform across the Southern Ocean. This is because the processes represented by the standard thermodynamic decay models are insufficient to simulate the observed deterioration of large icebergs; these icebergs circle the continent, slowly melting and delivering fresh water throughout the Southern Ocean. To highlight how unrealistic these simulations are, we note that 30% of the total fresh water is carried to latitudes lower than 40°S (outside of the simulated domain), whereas even the largest icebergs are rarely observed further north than 45°S (Fig. 1).

In a third set of simulations that have the breakup scheme active, the trajectories of large icebergs (Fig. 4C) correspond much better with the observations (Fig. 1). Note that we should not expect to match the trajectories of individual large icebergs; rather, we compare the

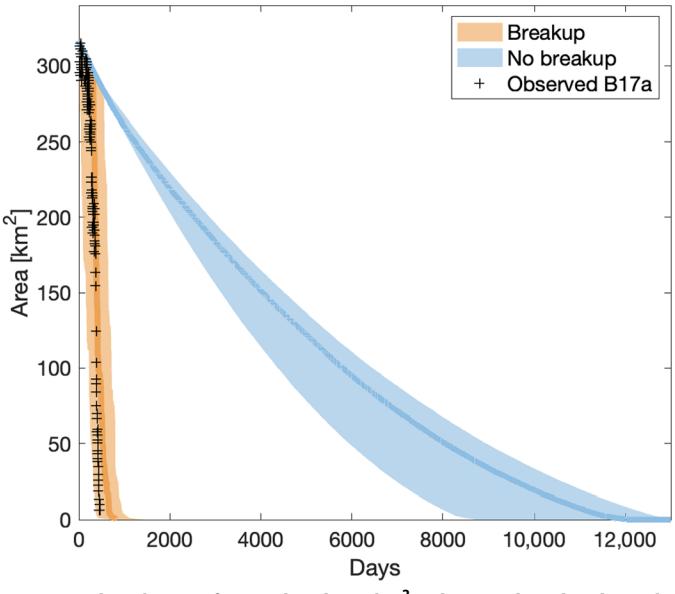

Fig. 3. Areal evolution of a simulated 300-km^2 iceberg with and without the breakup scheme compared to an observed iceberg. Evolution of the area of iceberg B17a [black crosses, from (*30*)], 10,000 icebergs simulated without representation of breakup (blue), and 10,000 icebergs simulated with the breakup scheme proposed here with $r = 4$ breakups/day (orange). The thick lines show the median value, and the shading indicates the interquartile range. Each iceberg enters the open ocean from the Weddell Sea region.

regions in which the icebergs terminate, as well as the overall pattern of the iceberg paths. Including the effects of fracturing has substantial implications for the meltwater distribution (Fig. 4F): Instead of an approximately uniform insertion of meltwater into the Southern Ocean (Fig. 4E), we find that the meltwater flux is concentrated in distinct regions of the Southern Ocean, namely, the region from the Weddell Sea into the South Atlantic sector and the region off of East Antarctica.

The majority of the meltwater entering into the South Atlantic sector of the Southern Ocean comes from the largest icebergs (300 to 1000 km^2; fig. S6). Many of these travel vast distances in the Antarctic Coastal Current without much decay before entering the Weddell Sea.

In contrast, the high concentration of meltwater flux close to East Antarctica mostly comes from the smaller icebergs (0.3 and 1 km^2; fig. S6) because they are more influenced by the winds (as described in WDE17) and so can break free from the ocean currents circling the continent.

From these results, we are able to examine the impacts of ignoring the breakup of large icebergs, or alternatively of ignoring large icebergs completely. Only considering small icebergs (Fig. 4D) injects a large amount of fresh water close to the coastline of Antarctica: In these simulations, 60% of the total fresh water is deposited within 100 km of the coastline. We speculate that this could potentially lead to an erroneous decrease in the production of Antarctic Bottom Water (*12*). On the other hand, including large icebergs but not including a mechanism for breakup spreads out the fresh water in the Southern Ocean too uniformly and transports it to low latitudes where icebergs are not observed. Therefore, these results suggest that to simulate the effect of icebergs on the Southern Ocean, it is critical to include both large tabular icebergs and a representation of their breakup beyond the standard decay models. To evaluate the specific effects on the Southern Ocean circulation and stratification, however, further work would be necessary with this breakup scheme implemented in a coupled ocean model.

DISCUSSION

In this study, we have used a model to investigate the importance of large tabular icebergs in distributing fresh water from Antarctica's glaciers and ice shelves. We focus on the effects of the fracturing of large icebergs, a dominant decay process that is not represented in standard iceberg decay models. Our results indicate that ignoring large tabular icebergs, as previous studies have typically done, leads to substantial differences in where fresh water is deposited into the Southern Ocean. In addition, we show that if large tabular icebergs are included but their decay is treated according to standard previous decay models that do not include breakup, then these large

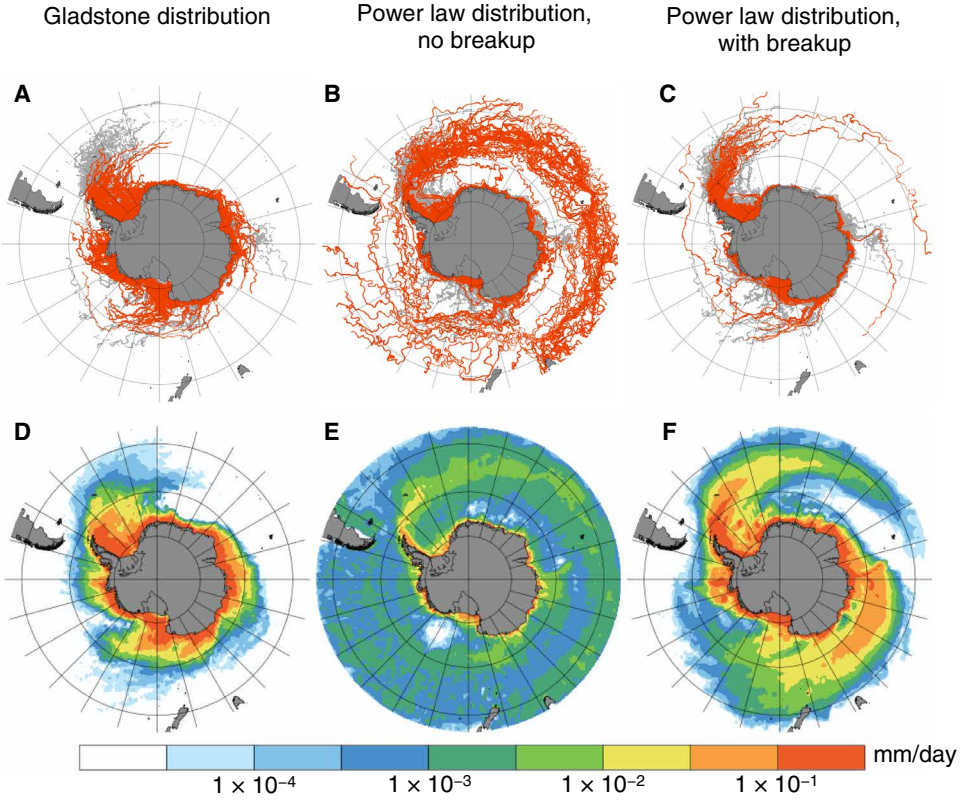

Fig. 4. Trajectories and freshwater distribution for the three sets of iceberg simulations. (Top) Trajectories and (bottom) meltwater flux from (**A** and **D**) only nontabular icebergs (Gladstone distribution), (**B** and **E**) the power law distribution with no breakup scheme, and (**C** and **F**) the power law distribution with the proposed breakup scheme included. For the trajectory plots, the child icebergs are not shown, and only the top four size classes are plotted in red, overlaid on the observed trajectories from Fig. 1 in gray. Note that the meltwater flux is scaled so that the total flux is the same for each set of runs (~1300 Gt/year) and that the meltwater flux is plotted on a log scale, in units of millimeter per day. All icebergs were simulated until they had fully melted (or a maximum of 40 years). Icebergs were seeded according to the calving distribution of Merino *et al*. (*8*) (fig. S1).

icebergs keep drifting for an unrealistically long amount of time and reach latitudes far equatorward of where icebergs are observed. We develop a physically based stochastic breakup scheme in which small icebergs calve from the larger tabular iceberg according to the footloose mechanism. We show that although most fresh water is injected by small icebergs, the large tabular icebergs are essential as they act as conveyor belts for the smaller icebergs, and their trajectories determine where these smaller icebergs are released and therefore where the fresh water will be distributed in the Southern Ocean. The resulting meltwater distribution has a notable spatial structure, with high-input regions in the Weddell Sea/South Atlantic region and the East Antarctic.

The largest tabular icebergs we simulated were 1000 km^2, which is more than 400× larger than most previous studies have examined. However, although relatively rare, there have been icebergs up to 10 times larger than this. We did not simulate these gigantic icebergs, as the proposed breakup scheme is insufficient to model their deterioration. Their observed initial decay is instead dominated by breakup from collisions with ice shelves and islands (*49*, *50*), a process not simulated in our model. Other processes that can lead to splitting of very large icebergs and are not accounted for here include swell-induced flexural breakup and hydrofracturing due to accumulation of meltwater on the iceberg surface. Although this is a limitation of our study, it is relatively rare for icebergs to emerge from the sea ice edge with an area larger than 1000 km^2; hence, the impact of this omission on the drift trajectories and freshwater distribution in the open ocean may be limited.

The aim of this study is twofold: (i) to provide a proof of concept that modeling the breakup of large icebergs leads to better agreement with observations and substantially influences the location where meltwater is injected, and (ii) to propose a breakup scheme that enables a physically meaningful representation of tabular icebergs in models.

The breakup scheme is relatively idealized and is based on several assumptions. For example, we have taken the probability of a child iceberg breaking from the parent iceberg to be constant in time (except in sea ice where the probability is set to zero). It is likely, however, that the probability depends on the roughness of the sea and the SST; both of these quantities influence the rate at which the wave-cut forms, which is the initial step in the footloose mechanism. In addition, although observations guided our choice [e.g., (*30*)], the breakup parameter r is only loosely constrained. The value of this parameter will likely have a substantial impact on the resulting iceberg meltwater flux distribution. One way to think about this is that if the probability of breakup is increased, the resulting meltwater distribution would look closer to the results for only small icebergs (Fig. 4D), whereas if the probability of breakup is decreased, the meltwater distribution would begin to resemble the results with the power law iceberg distribution with no breakup (Fig. 4E).

SUPPLEMENTARY MATERIALS

Supplementary material for this article is available at http://advances.sciencemag.org/cgi/content/full/6/51/eabd1273/DC1

REFERENCES AND NOTES

1. M. A. Depoorter, J. L. Bamber, J. A. Griggs, J. T. M. Lenaerts, S. R. M. Ligtenberg, M. R. van den Broeke, G. Moholdt, Calving fluxes and basal melt rates of Antarctic ice shelves. *Nature* **502**, 89–92 (2013).
2. E. Rignot, S. Jacobs, J. Mouginot, B. Scheuchl, Ice-shelf melting around Antarctica. *Science* **341**, 266–270 (2013).
3. J. Tournadre, N. Bouhier, F. Girard-Ardhuin, F. Rémy, Large icebergs characteristics from altimeter waveforms analysis. *J. Geophys. Res. Oceans* **120**, 1954–1974 (2015).
4. J. Tournadre, N. Bouhier, F. Girard-Ardhuin, F. Rémy, Antarctic icebergs distributions 1992-2014. *J. Geophys. Res. Oceans* **121**, 327–349 (2016).
5. J. I. Jongma, E. Driesschaert, T. Fichefet, H. Goosse, H. Renssen, The effect of dynamic–thermodynamic icebergs on the Southern Ocean climate in a three-dimensional model. *Ocean Model.* **26**, 104–113 (2009).
6. T. Martin, A. Adcroft, Parameterizing the fresh-water flux from land ice to ocean with interactive icebergs in a coupled climate model. *Ocean Model.* **34**, 111–124 (2010).
7. R. Marsh, V. O. Ivchenko, N. Skliris, S. Alderson, G. R. Bigg, G. Madec, A. T. Blaker, Y. Aksenov, B. Sinha, A. C. Coward, J. Le Sommer, N. Merino, V. B. Zalesny, NEMO-ICB (v1.0): Interactive icebergs in the NEMO ocean model globally configured at eddy-permitting resolution. *Geosci. Model Dev.* **8**, 1547–1562 (2015).
8. N. Merino, J. L. Sommer, G. Durand, N. C. Jourdain, G. Madec, P. Mathiot, J. Tournadre, Antarctic icebergs melt over the Southern Ocean: Climatology and impact on sea ice. *Ocean Model.* **104**, 99–110 (2016).
9. A. A. Stern, A. Adcroft, O. Sergienko, The effects of Antarctic iceberg calving-size distribution in a global climate model. *J. Geophys. Res. Oceans* **121**, 5773–5788 (2016).
10. D. Storkey, A. T. Blaker, P. Mathiot, A. Megann, Y. Aksenov, E. W. Blockley, D. Calvert, T. Graham, H. T. Hewitt, P. Hyder, T. Kuhlbrodt, J. G. L. Rae, B. Sinha, Uk Global Ocean GO6 and GO7: A traceable hierarchy of model resolutions. *Geosci. Model Dev.* **11**, 3187–3213 (2018).
11. T. Rackow, C. Wesche, R. Timmermann, H. Hellmer, S. Juricke, T. Jung, A simulation of small to giant Antarctic iceberg evolution: Differential impact on climatology estimates. *J. Geophys. Res. Oceans* **122**, 3170–3190 (2017).
12. V. Lago, M. H. England, Projected slowdown of Antarctic Bottom Water formation in response to amplified meltwater contributions. *J. Climate* **32**, 6319–6335 (2019).
13. F. Schloesser, T. Friedrich, A. Timmermann, R. M. DeConto, D. Pollard, Antarctic iceberg impacts on future Southern Hemisphere climate. *Nat. Clim. Change* **9**, 672–677 (2019).
14. S. J. Marsland, J.-O. Wolff, On the sensitivity of Southern Ocean sea ice to the surface freshwater flux: A model study. *J. Geophys. Res. Oceans* **106**, 2723–2741 (2001).
15. V. V. Menezes, A. M. Macdonald, C. Schatzman, Accelerated freshening of Antarctic Bottom Water over the last decade in the Southern Indian Ocean. *Sci. Adv.* **3**, e1601426 (2017).
16. A. M. Hogg, An Antarctic Circumpolar Current driven by surface buoyancy forcing. *Geophys. Res. Lett.* **37**, L23601 (2010).
17. M. Bügelmayer, D. M. Roche, H. Renssen, How do icebergs affect the Greenland ice sheet under pre-industrial conditions? – A model study with a fully coupled ice-sheet–climate model. *Cryosphere* **9**, 821–835 (2015).
18. H. Heinrich, Origin and consequences of cyclic ice rafting in the Northeast Atlantic Ocean during the past 130,000 years. *Quatern. Res.* **29**, 142–152 (1988).
19. W. S. Broecker, Massive iceberg discharges as triggers for global climate change. *Nature* **372**, 421–424 (1994).
20. T. J. W. Wagner, R. W. Dell, I. Eisenman, R. F. Keeling, L. Padman, J. P. Severing-haus, Wave inhibition by sea ice enables trans-Atlantic ice rafting of debris during Heinrich events. *Earth Planet. Sci. Lett.* **495**, 157–163 (2018).
21. Y. Liu, J. C. Moore, X. Cheng, R. M. Gladstone, J. N. Bassis, H. Liu, J. Wen, F. Hui, Ocean-driven thinning enhances iceberg calving and retreat of Antarctic ice shelves. *Proc. Natl. Acad. Sci. U.S.A.* **112**, 3263–3268 (2015).
22. F. Pattyn, M. Morlighem, The uncertain future of the Antarctic Ice Sheet. *Science* **367**, 1331–1335 (2020).
23. R. M. Gladstone, G. R. Bigg, K. W. Nicholls, Iceberg trajectory modeling and meltwater injection in the Southern Ocean. *J. Geophys. Res.* **106**, 19903–19915 (2001).
24. A. G. Pauling, C. M. Bitz, I. J. Smith, P. J. Langhorne, The response of the Southern Ocean and Antarctic sea ice to freshwater from ice shelves in an earth system model. *J. Climate* **29**, 1655–1672 (2016).
25. M. Kristensen, V. A. Squire, S. C. Moore, Tabular icebergs in ocean waves. *Nature* **297**, 669–671 (1982).
26. T. Scambos, O. Sergienko, A. Sargent, D. MacAyeal, J. Fastook, ICESat profiles of tabular iceberg margins and iceberg breakup at low latitudes. *Geophys. Res. Lett.* **32**, L23S09 (2005).
27. T. Scambos, R. Ross, R. Bauer, Y. Yermolin, P. Skvarca, D. Long, J. Bohlander, T. Haran, Calving and ice-shelf break-up processes investigated by proxy: Antarctic tabular iceberg evolution during northward drift. *J. Glaciol.* **54**, 579–591 (2008).
28. T. J. W. Wagner, R. Dell, I. Eisenman, An analytical model of iceberg drift. *J. Phys. Oceanogr.* **47**, 1605–1616 (2017).
29. J. S. Budge, D. G. Long, A comprehensive database for Antarctic iceberg tracking using scatterometer data. *IEEE J. Sel. Top. Appl. Earth Obs. Remote Sens.* **11**, 434–442 (2018).
30. N. Bouhier, J. Tournadre, F. Rémy, R. Gourves-Cousin, Melting and fragmentation laws from the evolution of two large Southern Ocean icebergs estimated from satellite data. *Cryosphere* **12**, 2267–2285 (2018).

31. T. Li, M. Shokr, Y. Liu, X. Cheng, T. Li, F. Wang, F. Hui, Monitoring the tabular icebergs C28A and C28B calved from the Mertz Ice Tongue using radar remote sensing data. *Remote Sens. Environ.* **216**, 615–625 (2018).
32. G. R. Bigg, M. R. Wadley, D. P. Stevens, J. A. Johnson, Modelling the dynamics and thermodynamics of icebergs. *Cold Reg. Sci. Technol.* **26**, 113–135 (1997).
33. J. Morison, D. Goldberg, A brief study of the force balance between a small iceberg, the ocean, sea ice, and the atmosphere in the weddell sea. *Cold Reg. Sci. Technol.* **76–77**, 69–76 (2012).
34. D. Menemenlis, J.-M. Campin, P. Heimbach, C. Hill, T. Lee, A. Nguyen, M. Schodlok, H. Zhang, Ecco2: High resolution global ocean and sea ice data synthesis. *Mercator Ocean Quart. Newslett.* **31**, 13–21 (2008).
35. D. L. Volkov, L.-L. Fu, T. Lee, Mechanisms of the meridional heat transport in the Southern Ocean. *Ocean Dyn.* **60**, 791–801 (2010).
36. M. P. Schodlok, D. Menemenlis, E. J. Rignot, Ice shelf basal melt rates around Antarctica from simulations and observations. *J. Geophys. Res. Oceans* **121**, 1085–1109 (2016).
37. M. Azaneu, R. Kerr, M. M. Mata, Assessment of the representation of Antarctic Bottom Water properties in the ECCO2 reanalysis. *Ocean Sci.* **10**, 923–946 (2014).
38. ERA5: Fifth generation of ecmwf atmospheric reanalyses of the global climate (2017); https://cds.climate.copernicus.eu/cdsapp/home.
39. J. Ramon, L. Lledó, V. Torralba, A. Soret, F. J. Doblas-Reyes, What global reanalysis best represents near-surface winds? *Q. J. Roy. Meteorol. Soc.* **145**, 3236–3251 (2019).
40. É. Vignon, O. Traullé, A. Berne, On the fine vertical structure of the low tro-posphere over the coastal margins of East Antarctica. *Atmos. Chem. Phys.* **19**, 4659–4683 (2019).
41. M. El-Tahan, S. Venkatesh, H. El-Tahan, Validation and quantitative assessment of the deterioration mechanisms of Arctic icebergs. *J. Offshore Mech. Arct. Eng.* **109**, 102–108 (1987).
42. I. Kubat, M. Sayed, S. Savage, T. Carrieres, G. Crocker. An operational iceberg deterioration model. In *Proceedings of the seventeenth international offshore and polar engineering conference* (The International Society of Offshore and Polar Engineers, 2007), pp. 652–657.
43. T. H. Jacka, A. B. Giles, Antarctic iceberg distribution and dissolution from ship-based observations. *J.Glaciol.* **53**, 341–356 (2007).
44. T. A. M. Silva, G. R. Bigg, K. W. Nicholls, Contribution of giant icebergs to the Southern Ocean freshwater flux. *J. Geophys. Res.* **111**, C03004 (2006).
45. J. A. Åström, Statistical models of brittle fragmentation. *Adv. Phys.* **55**, 247–278 (2006).
46. S. Savage, Geomophological Fluid Mechanics, chapter Aspects of iceberg drift and detioration (Springer, 2001).
47. T. J. W. Wagner, P. Wadhams, R. Bates, P. Elosegui, A. Stern, D. Vella, E. P. Abrahamsen, A. Crawford, K. W. Nicholls, The "footloose" mechanism: Iceberg decay from hydrostatic stresses. *Geophys. Res. Lett.* **41**, 5522–5529 (2014).
48. M. A. Lazzara, K. C. Jezek, T. A. Scambos, D. R. MacAyeal, J. C. van der Veen, On the recent calving of icebergs from the Ross Ice Shelf1. *Polar Geogr.* **23**, 201–212 (1999).
49. D. R. MacAyeal, M. H. Okal, J. E. Thom, K. M. Brunt, Y.-J. Kim, A. K. Bliss, Tabular iceberg collisions within the coastal regime. *J. Glaciol.* **54**, 371–386 (2008).
50. S. Martin, R. Drucker, R. Aster, F. Davey, E. Okal, T. Scambos, D. MacAyeal, Kinematic and seismic analysis of giant tabular iceberg breakup at Cape Adare, Antarctica. *J. Geophys. Res.* **115**, B06311 (2010).

Acknowledgments

Funding: This work was supported by NSF grants OPP-1744835 OPP-1643445. **Author contributions:** T.J.W.W. and I.E. conceived of the study. M.R.E. performed the simulations. All authors analyzed the results and contributed to the writing of the manuscript. **Competing interests:** The authors declare that they have no competing interests. **Data and materials availability:** All data needed to evaluate the conclusions in the paper are present in the paper and/or the Supplementary Materials. Additional data related to this paper may be requested from the authors. The code used in this study is available online at https://eisenman-group.github.io.

Submitted 2 June 2020
Accepted 21 October 2020
Published 16 December 2020
10.1126/sciadv.abd1273

Citation: M. R. England, T. J. W. Wagner, I. Eisenman, Modeling the breakup of tabular icebergs. *Sci. Adv.* **6**, eabd1273 (2020).

Science Advances

Modeling the breakup of tabular icebergs

Mark R. England, Till J. W. Wagner and Ian Eisenman

Sci Adv **6** (51), eabd1273.
DOI: 10.1126/sciadv.abd1273

Science Advances
AAAS

advances.sciencemag.org/cgi/content/full/6/51/eabd1273/DC1

Supplementary Materials for

Modeling the breakup of tabular icebergs

Mark R. England*, Till J. W. Wagner, Ian Eisenman

*Corresponding author. Email: mengland@ucsd.edu

Published 16 December 2020, *Sci. Adv.* **6**, eabd1273 (2020)
DOI: 10.1126/sciadv.abd1273

This PDF file includes:

Table S1: **Iceberg size classes for the widely used "Gladstone Distribution" (11), which includes only small icebergs.** The area, length (L), width (W), and height (H) are listed for each iceberg size class, as well as the fractional count of total icebergs and fraction of the total iceberg freshwater that falls within each size class.

Area [km^2]	**L [km]**	**W [km]**	**H [m]**	**Fraction [%]**	**Freshwater [%]**
0.0024	0.06	0.04	40	25	0.0
0.0067	0.10	0.067	67	12	0.1
0.027	0.20	0.133	133	15	1.0
0.061	0.35	0.175	175	18	3.6
0.17	0.5	0.333	250	12	9.5
0.33	0.7	0.467	250	7	10.8
0.54	0.9	0.6	250	3	7.6
0.96	1.2	0.8	250	3	13.4
1.71	1.6	1.067	250	3	23.9
3.23	2.20	1.47	250	2	30.1

Table S2: **Iceberg size classes for the "Power Law Distribution" created for this study, which includes both small and large Antarctic icebergs**. Column labels are as in Table S1. Adapted from (45).

Area [km^2]	**L [km]**	**W [km]**	**H [m]**	**Fraction [%]**	**Freshwater [%]**
0.3	0.69	0.46	175	53.7	0.6
1	1.22	0.82	200	20.6	0.8
3	2.2	1.4	225	11.6	1.7
10	3.9	2.6	250	6.5	3.3
30	6.7	4.6	275	3.7	6.5
100	12.3	8.2	300	2.1	12.7
300	21.8	14.5	325	1.2	24.9
1000	38.7	25.8	350	0.7	49.4

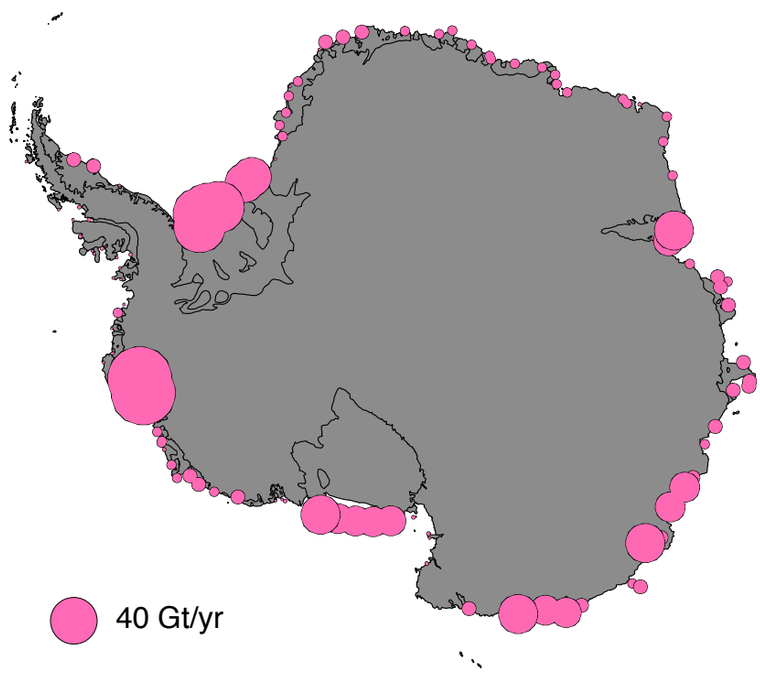

Figure S1: **Calving rates from Antarctic ice shelves**. For exact values, see supplementary data in ref. (29).

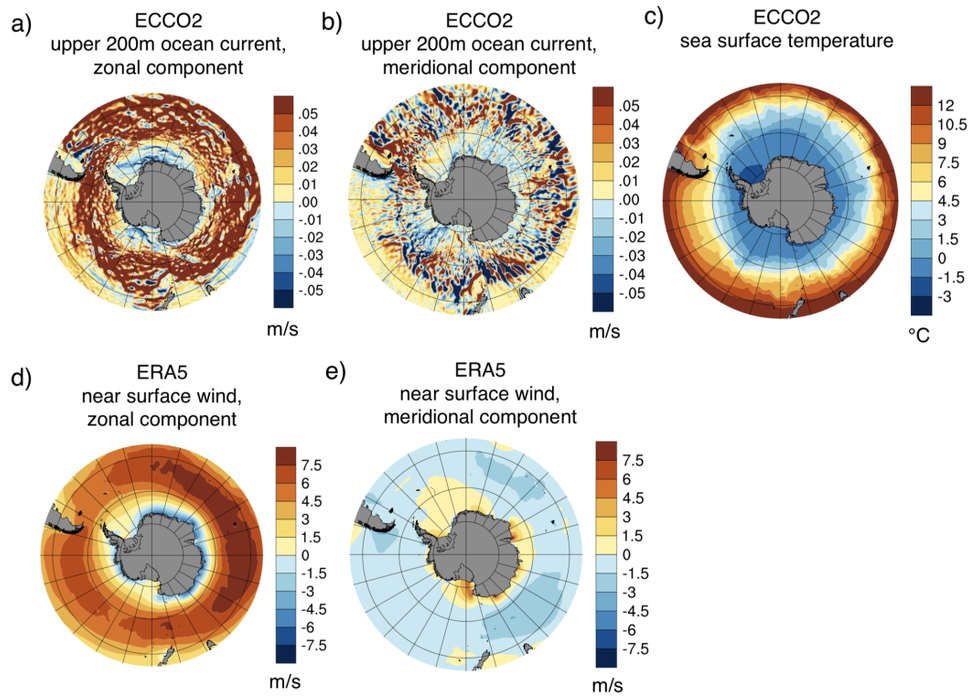

Figure S2: **Oceanic and atmospheric variables used to force the iceberg model.** Annual mean climatology from ECCO2 during 1992-2019 of the (a) zonal component and (b) meridional component of the upper-200m average ocean current, (c) sea surface temperatures and (e) sea ice concentration. Annual mean climatology from ERA5 during 1992-2019 of the (d) zonal component and (e) meridional component of the near surface wind field.

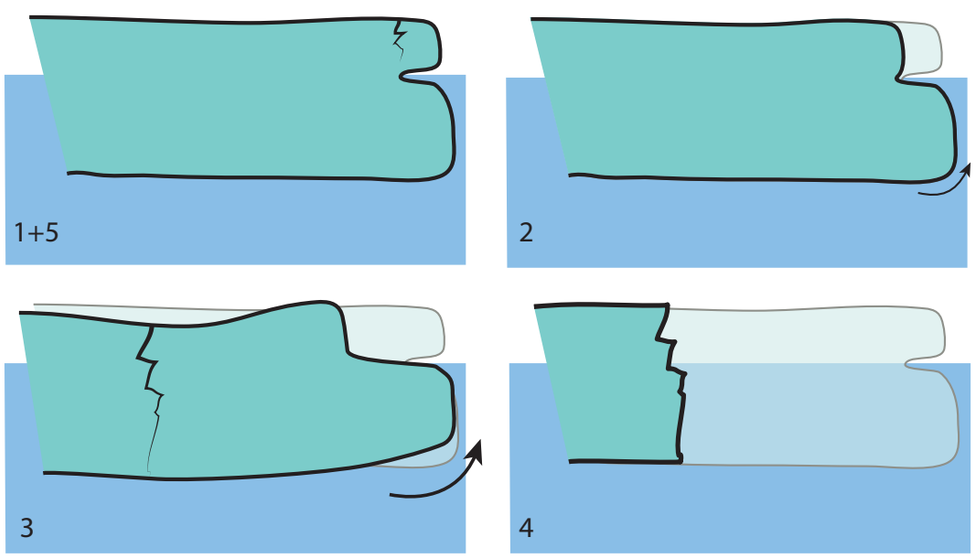

Figure S3: **Schematic of the "footloose mechanism".** Schematic of steps 1-5 of the "footloose" mechanism (48), described in Section 3 of the main text

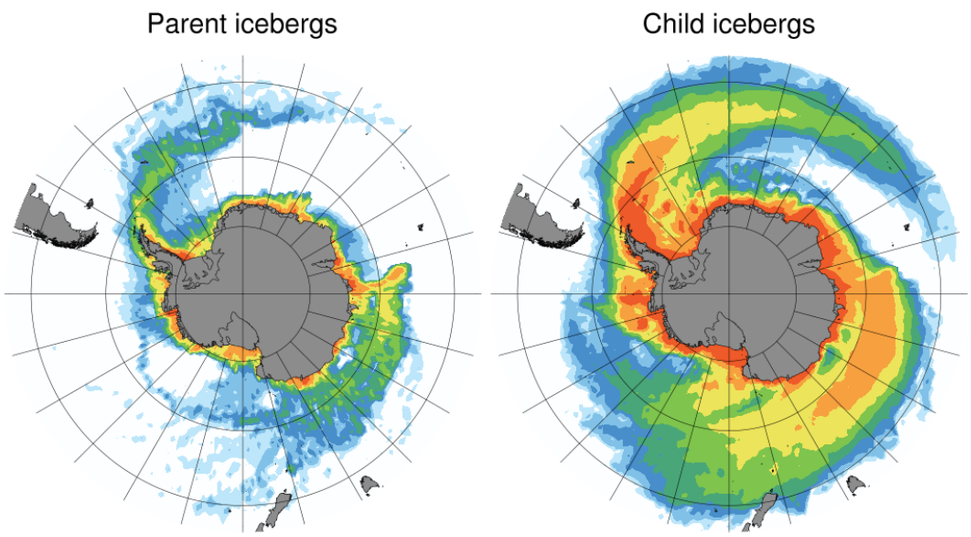

Figure S4: **Separating the simulated iceberg meltwater flux into contribution from and parent and child icebergs.** Meltwater flux from the (left) parent and (right) child icebergs in the simulation that uses the Power Law Distribution with the breakup scheme active using $r = 4$ breakups/day.

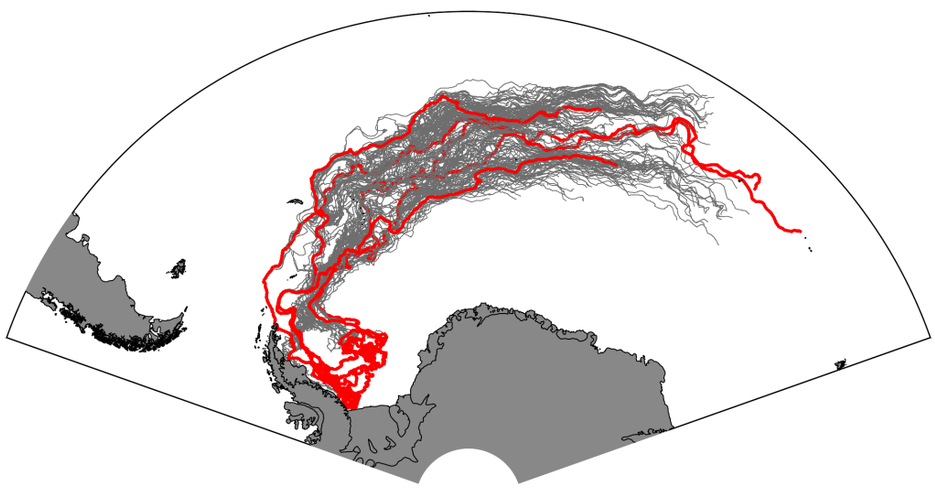

Figure S5: **Trajectories of five parent icebergs (red) released from the Weddell Sea Embayment together with the trajectories of their child icebergs (grey).** The child icebergs break off at a rate of $r = 4$ breakups/day.

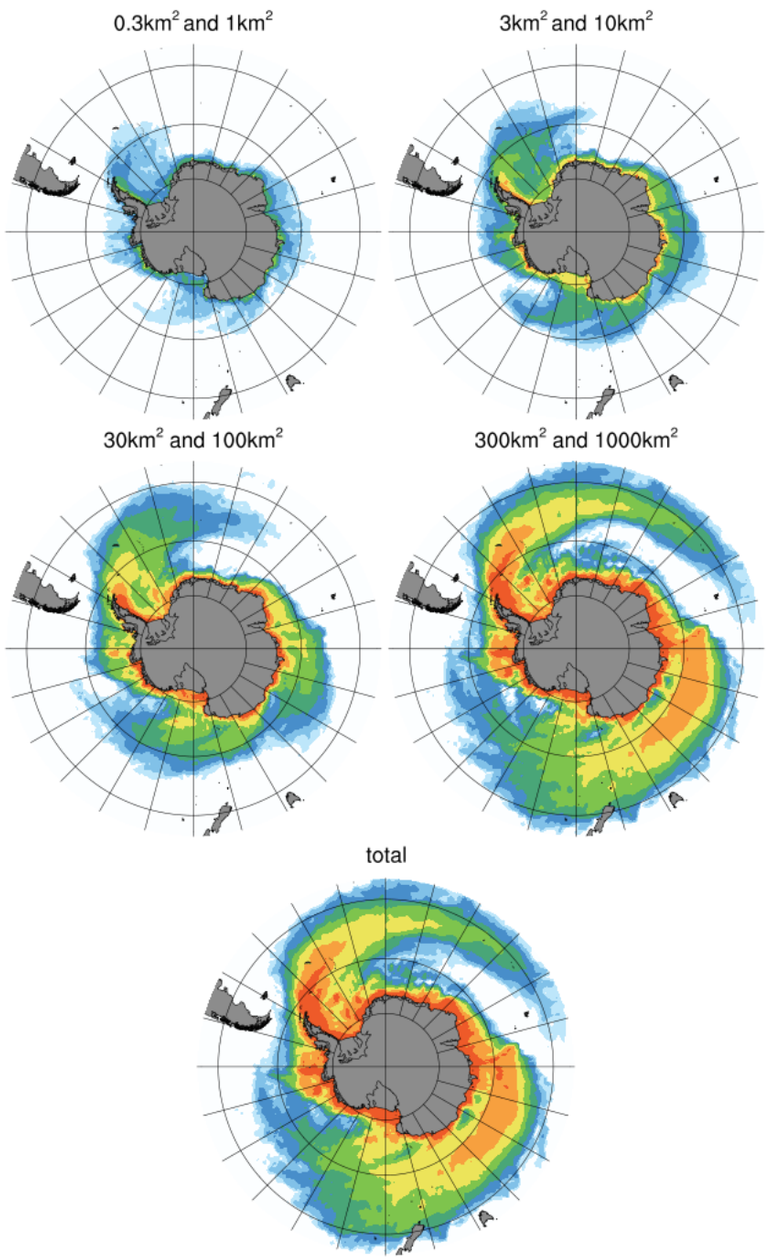

Figure S6: **Contribution of different iceberg size classes to simulated meltwater flux distribution.** Meltwater flux for runs with different iceberg size classes from the Power Law Distribution, with the breakup scheme active using $r = 4$ breakups/day. Here we have consolidated the size classes into pairs. The bottom panel shows the total.